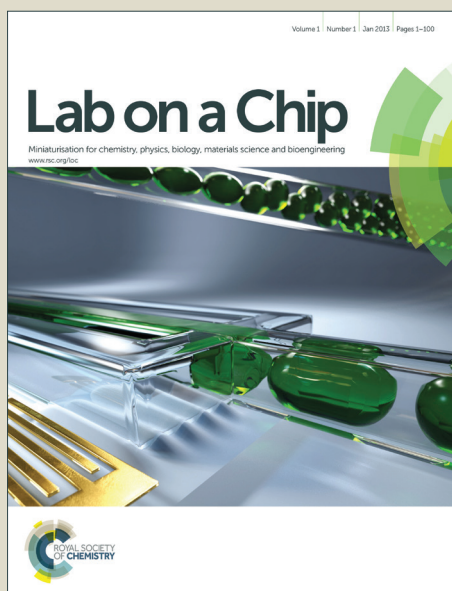


# Lab on a Chip

Accepted Manuscript



This is an *Accepted Manuscript*, which has been through the Royal Society of Chemistry peer review process and has been accepted for publication.

*Accepted Manuscripts* are published online shortly after acceptance, before technical editing, formatting and proof reading. Using this free service, authors can make their results available to the community, in citable form, before we publish the edited article. We will replace this *Accepted Manuscript* with the edited and formatted *Advance Article* as soon as it is available.

You can find more information about *Accepted Manuscripts* in the [Information for Authors](#).

Please note that technical editing may introduce minor changes to the text and/or graphics, which may alter content. The journal's standard [Terms & Conditions](#) and the [Ethical guidelines](#) still apply. In no event shall the Royal Society of Chemistry be held responsible for any errors or omissions in this *Accepted Manuscript* or any consequences arising from the use of any information it contains.

## ARTICLE

## Multiple Path Photonic Lab on a Chip for Parallel Protein Concentration Measurements

Isaac Rodríguez-Ruiz<sup>a</sup>\*, Mayte Conejero-Muriel<sup>b</sup>, Tobias N. Ackermann<sup>a</sup>, José A. Gavira<sup>b</sup> and Andreu Llobera<sup>a</sup>

Received 14th October 2014,  
Accepted 9th December 2014

[www.rsc.org/](http://www.rsc.org/)

We propose a PDMS-based photonic system for the accurate measurement of protein concentration with minute amounts of sample. As opposed to the state of the art, in the multiple path photonic lab on a chip (MPHIL), analyte concentration or molar absorptivity is obtained with a single injection step, by performing simultaneous parallel optical measurements varying the optical path length. Also, as opposed to the standard calibration protocol, MPHIL approach does not require a series of measurements at different concentrations. MPHIL has three main advantages: firstly the possibility of dynamically select the path length, always working in the absorbance vs concentration linear range for each target analyte. Secondly, a dramatic reduction of the total volume of sample required to obtain statistically reliable results. Thirdly, since only one injection is required, the measurement time is minimized, reducing both contamination and signal drifts. These characteristics are clearly advantageous when compared to commercial micro-spectrophotometers. The MPHIL concept was validated by testing three commercial proteins, Lysozyme (HEWL), Glucose Isomerase (D-xylose-ketol-isomerase, GI) and *Aspergillus* sp. Lipase L (BLL), as well as two proteins expressed and purified for this study, *B. cereus* formamidase (FASE) and dihydropyrimidinase from *S. meliloti* CECT41 (DHP). The use of the MPHIL is also proposed for any spectrophotometric measurement in the UV-VIS range, as well as for its integration as a concentration measurement platform in more advanced photonic lab on a chip systems.

### Introduction

The determination of protein concentration in solution is a routine measurement in many laboratories (biochemistry, molecular biology, structural biology, etc.). Precise determination of protein concentration becomes crucial for the calculation of other directly related parameters, such as enzyme activity, binding constant, etc. Therefore, any deviation in protein concentration measurement may lead to important errors in subsequent calculations and sample processing.<sup>1</sup> Solution concentration is generally determined by spectrophotometric detection, by different colorimetric assays (widespread methods are those proposed by Lowry,<sup>2</sup> Bradford,<sup>3</sup> and the use of bicinchoninic acid, BCA assay<sup>4</sup>), or by direct UV spectroscopy. In the aforementioned context, the reduction of sample volume is constantly sought due to the lack of sample produced with much effort and time for the cloning, expression and purification. For that reason, the use of UV spectroscopy

detection, in spite of being the most likely to produce inaccurate results,<sup>1</sup> has become widespread due to its simplicity and quick application, being also the less expensive method for determining protein concentration in terms of time and protein consumption.

In the last decade, the appearance of microfluidics, and specially of the micro-total analysis systems ( $\mu$ -TAS)<sup>5</sup> concept has favored a revolutionary environment for biochemistry and molecular biology, where the easy handling of small protein volumes has provided very powerful tools, not only for their study,<sup>6</sup> but also for other different purposes, ranging from sensing applications<sup>7</sup> to the performance of enzymatic biocatalytic reactions.<sup>8</sup> In this context, integrated optical detection systems have been merged with the  $\mu$ -TAS concept, giving birth to a new technological/scientific area in which the so called "photonic lab on a chip, PhLoC"<sup>9</sup> (allowing in situ spectrophotometric measurements in tiny amounts of sample) are in continuous development. Hitherto, this concept has

proven to be mature enough so as to report systems suitable to work in either absorbance,<sup>10, 11</sup> fluorescence<sup>12</sup> or scattering<sup>13, 14</sup> using samples from biological origin (including cell cultures). Nevertheless, to the best of our knowledge, most of the presented PhLoCs (and specially these based on absorbance) have a specific and fixed optical path, which restrains the linear range of the PhLoC depending on the molar absorptivity of the sample to be measured. In addition, analyte concentration is usually determined by means of a calibration curve (performed to determine the molar absorptivity of the analyte as well as the sensitivity and limit of detection of the system), which is done sequentially in these PhLoCs, by injecting and measuring samples of known analyte concentration. This clearly requires a significant processing time, as well as using a considerable amount of analyte. In addition, capturing air bubbles between two consecutive injections frequently occurs, being then necessary to empty the PhLoC, remove the air bubble, obtain again the reference spectrum and start the calibration from scratch. This situation comes along with the concomitant requirement of a much larger sample volume. In this context, systems allowing multiple parallelization of optical measurements would potentially present an extraordinary opportunity to increase throughput and efficiency, providing with more reliable results in terms of statistic data treatment and system robustness while reducing sample volumes and processing time, thus becoming clearly advantageous when compared to current commercial microspectrophotometers or the state of the art in PhLoC.

In this work we propose an on-chip “multiple path” PhLoC, hereafter referred as MPHIL, which has specially been designed for allowing multiple parallelization of optical measurements on a single sample. In addition, the proposed design presents an unconventional method for accurately determining protein concentration, requiring minute amounts of sample for the measurement. Therefore it can be used for any colorimetric assay in the UV-VIS spectra, being affordable to any laboratory due to its ease of fabrication by simple cast molding of (poly)dimethylsiloxane (PDMS).

## Experimental

### Materials and reagents

PDMS PDMS Sylgard 184 elastomer kit was supplied by Dow Corning (Midland, MI, USA). SU-8 polymer and propylene glycol methyl ether acetate developer (PGMEA) for MPHIL master fabrication were supplied by MicroChem, Corp. (Newton, MA, USA).

Lysozyme (HEWL) was purchased as a lyophilized powder from Sigma (L6876) and dissolved in 50 mM Sodium Acetate pH 4.5. Glucose isomerase (D-xylose-ketol-isomerase, GI) was purchased as a crystal suspension from Hampton Research (HR7-100). Crystals were dissolved in water and extensively dialyzed against 100 mM Hepes pH 7.0. *Aspergillus sp.* lipase L (BLL) was purchased from Biocon (Spain) (L8410) and dialyzed against water. *Bacillus cereus* formamidase (FASE)

and dihydropyrimidinase from *S. meliloti* CECT41 (DHP) were expressed in *E. coli* BL21 (DE3) as a fusion protein with a C-terminal hexahistidine tag and purified from bacterial lysates by affinity chromatography (15ml bed volume, GE Healthcare) and a Superdex 200 size exclusion column (GE Healthcare) in 50 mM Na<sub>2</sub>HPO<sub>4</sub> and 300 mM NaCl. Based on SDS-PAGE experiments, the purity of the recombinant protein was estimated to be greater than 95%. FASE and DHQ were dialyzed overnight against 20 mM Tris buffer pH 8.0 and concentrated using a Centricon centrifugation system with a 10 kDa molecular weight cutoff membrane.

### Design and concept

The MPHIL prototype, depicted in Figure 1, consists of a serpentine channel describing 6 different optical paths (OP) with lengths varying from 0.05 to 1 cm (L<sub>1</sub> to L<sub>6</sub>). The number of the OPs was chosen as a compromise between having a statistically significant number of measurements with the minimal amount of sample required (injected in a single step).

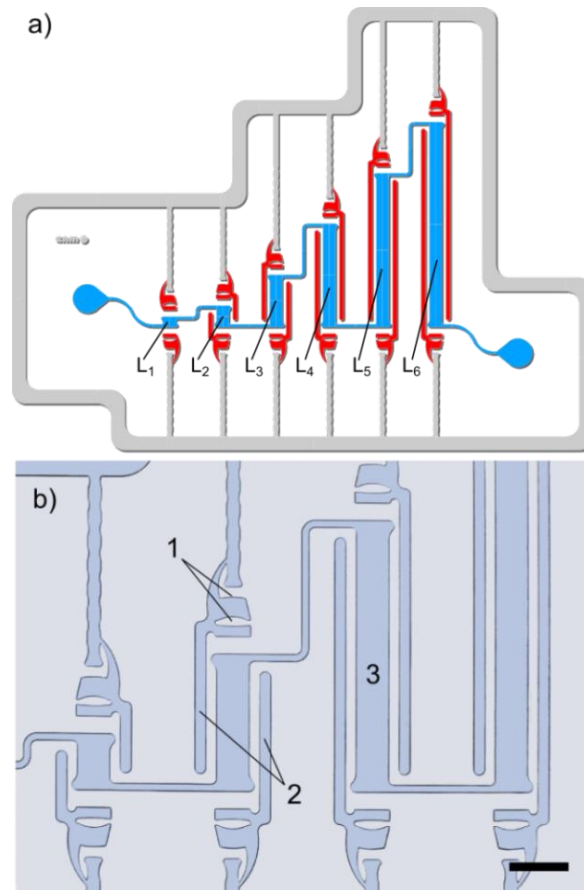


Figure 1: a) Schematic of the MPHIL (blue: fluidic channel, red: optical elements); It consists on a serpentine channel describing 6 different optical paths (OP), with lengths from 0.05 to 1 cm (L<sub>1</sub> to L<sub>6</sub>). 2D microlenses and fiber optics channels can also be seen at each end of the OP b) Detail of a fabricated MPHIL. 1: 2D microlenses; 2: air mirrors to prevent cross talking; 3: interrogation channel. Scale bar = 1 mm.

As commented in the introduction section, the MPHIL presents an unconventional method for determining concentrations in

solution: as opposite to the state of the art, this system is based in multiple parallel measurements on a single sample at constant concentration, varying the optical path length ( $L_i$ ). This “multiple path” configuration permits an increase in the linearity range, which relates concentration and absorbance (absorbance values from 0 to 1 A.U.) in accordance to the Beer-Lambert law,

$$A_i = \epsilon L_i C \quad (1)$$

where  $A_i$  and  $L_i$  (cm) ( $i=1, \dots, N$ ) are the absorbances and the optical paths implemented in the MPHIL (at a fixed wavelength),  $\epsilon$  is the molar absorptivity ( $M^{-1} \text{ cm}^{-1}$ ) and  $C$  is the concentration of the analyte (M). The deviation from the linearity postulated by the Beer Lambert law is commonly observed for high analyte concentrations for a fixed  $L$  value, due to the change in refractive index of the solution, which is not considered in the Beer Lambert law derivation. From eq. (1) it is evident that the shortening of the optical path leads to the decreasing of the absorbance signal. Hence, the possibility of simultaneously exploring different path lengths ( $L_i$ ) can be correlated with a more efficient measurement in terms of time and reagent consumption if considering a situation where, for a given analyte and using a given optical path,  $L_m$ , absorbance values over 1 A.U. were obtained. Under these conditions, either sample dilution or reduction of the optical path (meaning a change in the design and a new fabrication process) would be required. In the MPHIL, without requiring sample extraction, simply by selecting another optical path  $L_n$  ( $< L_m$ ) it would be possible to retrieve absorbance measurements in the linear range.

Optical interrogation channels, comprising a self-alignment element for accurate fiber optics positioning (see Figure 1) and a set of 2D microlenses that modulate the light beam to optimize light-analyte interaction were located at each optical path. Channel depth was selected to permit the insertion and positioning of 230  $\mu\text{m}$  diameter fiber optics, leading to a total system volume of  $< 3 \mu\text{L}$ . The set of micro-lenses is made of the same material as the walls of the channels (PDMS), and defined according to the refractive index of PDMS ( $n_{\text{PDMS}} = 1.41$  at  $\lambda = 633 \text{ nm}$ )<sup>15</sup> and air ( $n_{\text{air}} = 1$ ) to collimate the light beam passing across the interrogation channels. The microlenses were designed to allow the closest proximity of the fiber optics to the interrogation channel while maintaining collimation and minimizing intensity losses in the visible spectrum. In addition, air mirrors<sup>16</sup> were located at both sides of the optical path with a two-fold function: from one side, it allowed light confinement in the optical path, from the other side, did not allow light from a different optical path to couple to the output microlens, reducing thus the crosstalk between adjacent OP.

### Photonic simulations

The ray tracing simulations for the design of the micro-optical elements were performed using TracePro software (Lambda Research Corporation, Littleton, USA). Fiber optics with 200

$\mu\text{m}$  core diameter (230  $\mu\text{m}$  cladding diameter) and numerical aperture of 0.22 were implemented using the respective refractive indices of core and cladding. The simulations were performed tracing 67051 rays and defining a fixed initial flux per ray. Figure 2 presents a screenshot of the simulation of the light propagating along one of the MPHIL optical paths, describing the performance of the air mirrors, avoiding cross talking and confining light rays propagating along the MPHIL. Here, PDMS and air were considered transparent, whereas an arbitrary absorption coefficient was selected for the medium inside the fluidic channel in order to show the effect of absorption in the simulated rays. Only rays reaching the end of the output fiber optics were displayed for the sake of clarity when depicting the propagation of light contributing to the signal. The energy loss of the rays (each colour corresponds to the fraction of initial flux each ray carries: 1 - 0.66 = red; 0.66 - 0.33 = green, 0.33 - 0 = blue) during propagation is caused by two factors, namely the absorption of the medium and Fresnel reflection at the different interfaces.

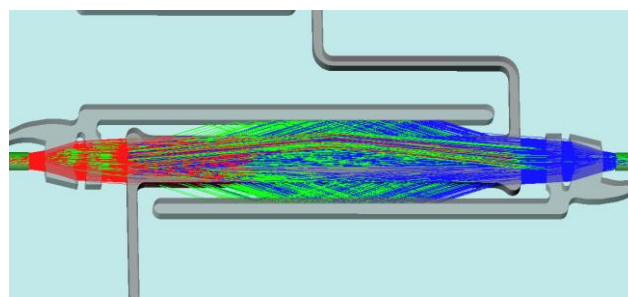


Figure 2. Screenshot of a ray tracing simulation across one MPHIL OP, illustrating the performance of the included micro-optical elements (air mirrors and microlenses).

### Validation of the numerical results

Numerical simulation of an OP including microlenses and air mirrors is shown in Figure 2. As can be observed, light is simulated to be injected from a multimode fiber optics with a Numerical Aperture (NA) of 0.22. After the first microlens, the beam divergence is corrected and most of the rays enter the analysis region parallel to its axis<sup>16</sup>. Those rays with a given propagation angle reach, after a certain propagation length, the liquid/PDMS interface. Due to the low Fresnel reflection coefficient, a fraction higher than 99% is coupled into the PDMS and can only be reflected back to the analysis region inserting an air mirror, which in addition shields each OP. Numerical simulations have shown that cross-talk between adjacent optical paths is close to 27 dB. Such numerical results were validated by visualizing the light propagation through an OP comprising a microfluidic channel filled with a saturated fluorescein solution excited with a 405 nm laser and the collimation microlens. A screenshot of the performed ray tracing simulations for the microlenses, together with the fluorescence image of the collimated light beam is presented in Figure 3 with the aim of comparison. In this case, only red rays are displayed in the simulation (Figure 3a), as they carry the

major part of the energy. Figure 3b shows how the light propagating through the channel filled with the saturated fluorescein solution has small divergence in accordance with the numerical simulation depicted in Figure 3a.

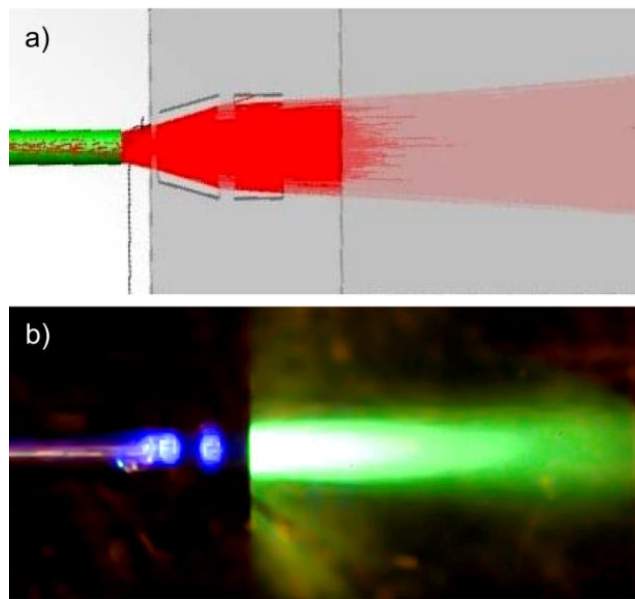


Figure 3. a) Lens ray tracing simulations considering the refractive index of PDMS ( $n_{\text{PDMS}} = 1.41$  at  $\lambda = 633$  nm)<sup>15</sup> and air ( $n_{\text{air}} = 1$ ) performed with TracePro software; b) fluorescence image of the collimated light beam in an OP comprising a microfluidic channel filled with a fluorescein saturated solution, excited with a 405 nm laser

### MPHIL fabrication

The MPHIL concept was validated with the fabrication of an on-chip prototype by casting of PDMS in a SU-8 master, manufactured by soft lithography. The fabrication process for the SU-8 masters has been previously reported,<sup>10</sup> but it is briefly described here for completeness. A silicon wafer was used as a substrate and dehydrated at 200 °C for 1 h prior to the spinning of an SU-8 layer with a thickness of 5  $\mu\text{m}$  (which acts as a seed layer to increase the adhesion of subsequent SU-8 layers). Afterwards, the substrate was baked at 95 °C for 30 minutes and flood exposed to UV light. A post-exposure bake (PEB) at 95 °C was followed, subsequently slowly cooling down to room temperature, in order to avoid any crack in the layer due to temperature stress. Then, with a single spin-on process using SU-8 2050, a thickness of 250  $\mu\text{m}$  was obtained, in order to reach a sufficient height that allowed a hassle-free insertion of the optical fibers. Then, an UV exposure with a mask that defined the OFS was followed by another PEB and development of the structures in PGMEA, finishing the definition of the master. Finally, the wafer was hard baked (HB) for 2 h at 120 °C under inert atmosphere to mechanically relax all the structures and eliminate possible micro-fractures, with the purpose of increasing the master long term stability.

PDMS pre-polymer was poured and cured over the SU-8 master on a hot plate at temperatures over 80 °C. It is known that PDMS suffers of shrinkage when the curing process is

accelerated by increasing the temperature.<sup>17, 18</sup> Consequently, a 10% of shrinkage in the MPHIL structure was considered for the calculation of the final MPHIL dimensions.

### Concentration measurement strategy

The system was tested by determining the molar absorptivity of the three commercial proteins, Lysozyme (HEWL), Glucose Isomerase (D-xylose-ketol-isomerase, (GI) and *Aspergillus sp.* lipase L (BLL), as well as two proteins expressed and purified for this study, *B. cereus* formamidase (FASE) and dihydropyrimidinase from *S. meliloti* CECT4114 (DHP). It is accepted that the absorbance of a protein (at  $\lambda = 280$  nm) depends on the content of three amino acids: tryptophan (Trp), tyrosine (Tyr) and cystine (Cys) groups (disulfide bonds). In addition, the molar absorptivity at the working wavelength  $\epsilon_{280}$  ( $\text{M}^{-1} \text{cm}^{-1}$ ) for a given protein follows the empirical equation:<sup>19</sup>

$$\epsilon_{280} = [\text{Trp}](5500) + [\text{Tyr}](1490) + [\text{Cys}](125) \quad (2)$$

where [Trp], [Tyr] and [Cys] values correspond to the number of residues of each type in the protein.

Absorbance measurements at  $\lambda = 280$  nm were obtained from single injections in the MPHIL using concentrations in the  $\mu\text{M}$  range, and using as the reference the buffer in which each protein was prepared. DH-2000 Mikropack Deuterium-Tungsten Halogen Light Source (Ocean Optics, Dunedin, FL, USA, USA), emitting at wavelengths ranging from 215 nm to 2000 nm was coupled to a multimode fiber optics with a diameter of 230  $\mu\text{m}$ , (Thorlabs, Dachau, Germany), which was located in the self-alignment microchannels. Light emerging from the MPHIL was coupled to an identical fiber optics, directly connected to an Ocean Optics MAYA 2000 spectrophotometer (Ocean Optics, Dunedin, FL, USA). Such configuration enables obtaining the spectral response in the UV-VIS range for any solution injected in the MPHIL. A conventional Cary 300 UV-VIS spectrophotometer (Agilent technologies, Santa Clara, CA, USA) was used for benchmarking the proposed MPHIL against standardized protocols. Experiments were performed a minimum of three times to carry out statistical analysis.

## Results and discussion

### Spectrophotometric measurements

The calculated  $\epsilon_{280}$  values for the 5 proteins, together with their molecular weight and number of absorbance contributors (Trp, Tyr and Cys) are summarized in Table 1, together with the measured molar absorptivity ( $\epsilon_{\text{M}}$ ) for the three commercial proteins, using the MPHIL approach. A high degree of correlation between measured and calculated values can be observed for the three proteins. In addition and relying in the values of  $\epsilon_{280}$  presented in Table 1, different concentrations of FASE and DHP proteins were determined as well. Figure 4 represents the performed absorbance measurements as a function of the optical path,  $L$ , displaying the linear relation

between both values, in accordance with equation (1). Protein concentrations were selected to present an absorbance below 1 A.U. in the largest optical path of the MPHIL ( $L_6$ ): This optimal situation allows using the 6 different optical paths for the measurements.  $R^2$  coefficients calculated from the least squares linear fitting of the data, (also represented in Figure 4 together with the measured values, averaged from a minimum of 3 experiments and presented with their standard deviation), show a very good correlation degree for all the measured concentrations.

Table 1. Main composition of the different measured proteins and their respective calculated and measured molar absorptivity ( $\epsilon_M$ ) values.

Acronym	MW*	Trp* (%)	Tyr* (%)	Cys* (%)	$\epsilon_T^*$	$\epsilon_M^*$
HEWL	14313	6 (4.7)	3 (2.3)	8 (6.2)	38.47	$36 \pm 5$
GI	43199	6 (1.5)	9 (2.3)	1 (0.3)	46.53	$45 \pm 4$
BLL	33456	5 (1.6)	16 (5.2)	6 (2.0)	52.09	$51 \pm 2$
FASE	38633	9 (2.6)	19 (5.5)	6 (1.7)	78.56	-
DHP	53433	8 (1.6)	11 (2.2)	6 (1.2)	61.14	-

\*MW ( $\text{g mol}^{-1}$ ); Trp, Tyr, Cys, number of amino acids present in the proteins and global percentage;  $\epsilon_T$  and  $\epsilon_M$ : theoretical and measured  $\epsilon$  ( $\text{M}^{-1} \text{cm}^{-1}$ )  $\times 10^{-3}$  values, respectively at the working wavelength of 280 nm

Obtained  $R^2$  values are presented in Table 2, together with FASE and DHP concentrations determined by the “multiple path” method. With the aim of comparison, these values are also benchmarked in Table 2 against concentration values obtained with a standard spectrophotometer (Cary 300). The agreement between the results and the reference values validates the MPHIL and the multiple path concept for analytes concentration determination, newly introduced in this work.

Table 2. Concentration measurements performed in the OFS with the “multiple path” method together with reference values obtained by conventional spectrometer and  $R^2$  values of the least squares linear fitting.

Acronym	[C] reference ( $\mu\text{M}$ )	[C] measured ( $\mu\text{M}$ )	$R^2$
FASE	$7.54 \pm 0.01$	$7.0 \pm 0.7$	0.98
	$9.37 \pm 0.02$	$9.2 \pm 0.5$	0.990
	$11.60 \pm 0.04$	$11.6 \pm 0.9$	0.98
DHP	$8.37 \pm 0.03$	$8.5 \pm 0.3$	0.98
	$14.03 \pm 0.09$	$14.1 \pm 0.2$	0.998
	$18.0 \pm 0.1$	$18.2 \pm 0.3$	0.9995

However, although the validation has been achieved through the comparison of static measurements of protein concentration, the idea behind the MPHIL and the multiple path method goes beyond a standard spectrometer. While many commercial microspectrometers for measuring protein concentration work with a single wavelength ( $\lambda = 280 \text{ nm}$ ) measuring static volumes, the MPHIL can also be conceived as a tool to be implemented and used as a multispectral detection component in more complex lab on a chip systems, where the different multiple paths would permit both detection and quantification of the target analytes. Moreover, due to its specific design (a

serpentine channel), the system is able to operate, not only with static volumes, but also in continuous flow regime, making it a good candidate to be used as a detection system for continuous sensing applications.

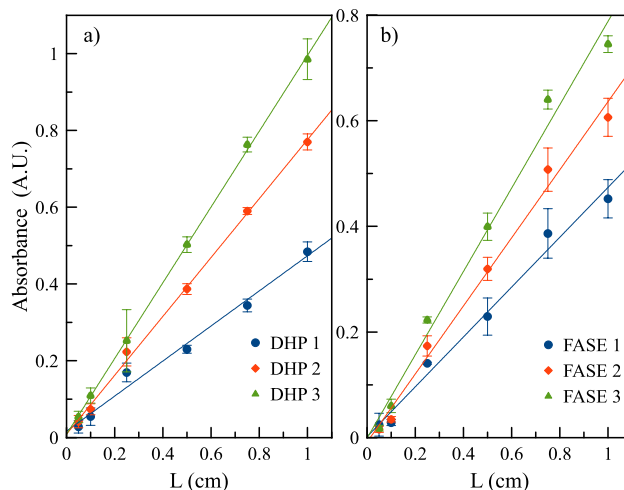


Figure 4. Absorbance measurements (in absorbance units, A.U.) vs optical path length ( $L$ ) performed with 3 different concentrations for DHP (a) and FASE (b) proteins, as a function of the optical path length ( $L$ ). DHP 1 =  $8.37 \pm 0.03 \mu\text{M}$ , DHP 2 =  $14.03 \pm 0.09 \mu\text{M}$ , DHP 3 =  $18.0 \pm 0.1 \mu\text{M}$ , FASE 1 =  $7.54 \pm 0.01 \mu\text{M}$ , FASE 2 =  $9.37 \pm 0.02 \mu\text{M}$ , FASE 3 =  $11.60 \pm 0.04 \mu\text{M}$ .

It is noteworthy that, as direct UV spectroscopy is the less adequate assay for measuring protein concentration in terms of accuracy, it presents an ideal condition for evaluating the sensitivity of the MPHIL in the worst possible scenario. Therefore, in view of the obtained results, there are some features of the proposed prototype that can be improved and are worth to be discussed.

These features to be considered are the construction material, PDMS, the light source used for the experiments and the selected range of optical paths as well, all affecting the sensitivity of the MPHIL. With respect to PDMS, it is well known for displaying a high transparency in the visible spectra, making it a good candidate for white light spectroscopy. Notwithstanding, its transmittance decreases up to 60% when approaching to UV wavelengths, having a lower limit for wavelengths below 250 nm. Considering that light only propagates inside the PDMS a total distance of 1.43 mm for any of the optical paths (this longitude has been measured considering the micro-lens, the fiber optics stopper at the end of the self-alignment element and the safety distance between the lens and the microfluidics to avoid leakage), even if the transmittance is decreased by 40% at low wavelengths, measurements could still be performed. Nonetheless the MPHIL concept is not restricted to PDMS, but other materials showing a higher transparency in the UV range may be used if required. Variation among obtained values in the same experimental conditions (measurements at constant  $C$  and  $L$ ) can also be observed. This can be explained as the sum of the effects of experimental errors (due to presence of impurities in the optical path, slight modification of fiber optics positioning

among measurements, and any other undetermined source of error), together with the characteristic emission spectrum of the light source employed in these experiments. As depicted in Figure 5, the emission spectrum displays an inflection point at 280 nm due to the existence of (at least) two intensity emission peaks at  $\lambda \approx 268$  nm and  $\lambda \approx 285$  nm. Any small deviation caused by experimental error can be dramatically magnified when measuring absorbance near this inflection point. Indeed, related to this appreciation, it can be observed in Figure 4 that deviations in FASE absorbance measurements are generally larger than those observed for DHP. This is explained taking into account its higher content in disulfide bonds resulting in a higher theoretical estimation of the molar absorptivity at  $\lambda = 280$  nm and consequently translated in larger deviations when compared with experimental measurements.

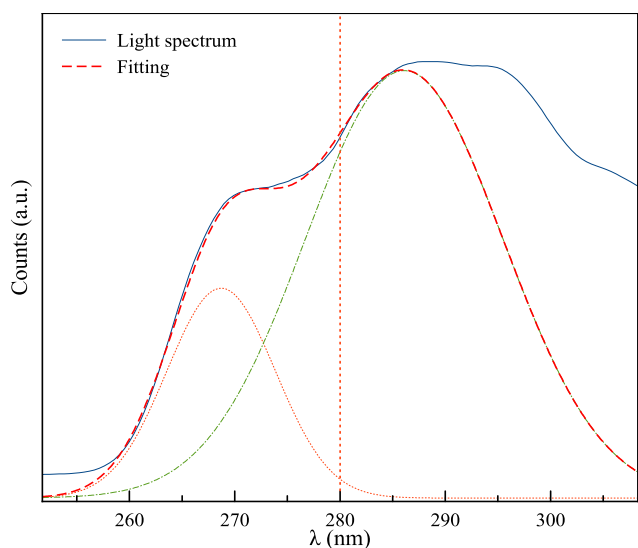


Figure 5. Emission spectrum of the light source used in the experimental setup. Red dotted vertical line at  $\lambda \approx 280$  nm shows the wavelength at which absorbance measurements were performed. An inflection point from the sum of emission peaks is observed. Light spectrum was deconvoluted in the region of interest to determine the location of two peaks at  $\lambda \approx 268$  and  $\lambda \approx 285$  nm, represented in dotted red and green lines respectively.

On the other hand, it becomes necessary to reach a compromise between reagent consumption and sensitivity of the system. It is plausible to assume that the shorter the optical path is, the lower the sensitivity of the measurements would be, though the contrary (i.e. the longer the optical path, the higher sensitivity) does not apply ad infinitum, as there are other factors to take into account i.e.: the beam broadening inherent of using cylindrical microlenses. Besides, large  $L$  values involve higher reagent consumption, which is against the MPHIL concept. To determine optimal design conditions for future MPHIL prototypes, the concept of limit of detection (LOD, using a  $k$  value of 3, ensuring a confidence level of 99.87 %) <sup>20</sup> was applied to determine a minimum  $L$  ensuring enough sensitivity to measure protein concentration in the studied ranges, and by direct UV spectroscopy. LOD is usually expressed as the concentration value (or amount), derived from the smallest

measure that can be detected with reasonable certainty for a given analytical procedure. Nevertheless, using the definition of LOD it is possible to determine a limit value for the optical path lengths as well. Calculations for this purpose were performed using GI as a model for the determination, and representing absorbance measurements as a function of different protein concentrations for each optical path. Figure 6a shows this representation for optical path values from 0.1 to 1 cm. All fittings displayed a good correlation ( $R^2 > 0.9$ ) except the one corresponding to the shortest optical path (0.05 cm), showing inconsistency among the other measured absorbance values. For that reason this value has been excluded from the graphical representation and further calculations. From this plot, LOD values between  $1.28 \pm 0.04$   $\mu\text{M}$  (L5) and  $8 \pm 2$   $\mu\text{M}$  (L2) were obtained for the GI. Aside, representing the analytical sensitivity (the slope of each linear fitting),  $S$ , as a function of the optical path (Figure 6b) it is possible to determine a limit path length by performing a linear fitting analysis, obtaining a value of  $L = (9.9 \pm 0.5) \times 10^{-2}$  cm. This limit path length value is presented as an orientative estimation, and extrapolating the LOD concept, will correspond to the minimum path length which would provide a measurable absorbance signal for the range of the studied GI concentrations. Important is to mention that this value is in accordance with our observations, as we did not obtain reliable measurements in optical paths under 0.1 cm.

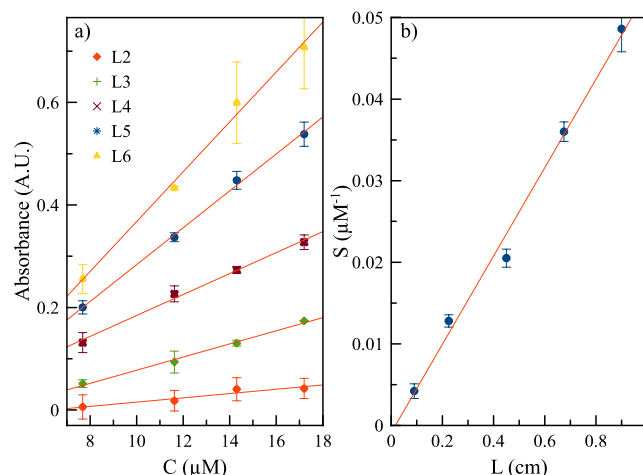


Figure 6. a) Plot of the absorbance measurements (in absorbance units, A.U.) as a function of different protein GI concentrations for each MPHIL optical path; b) Plot of the analytical sensitivity,  $S$ , as a function of optical path length. From the linear regression analysis of this plot it is possible to calculate a limit path length of  $L = (9.9 \pm 0.5) \times 10^{-2}$  cm.

Finally, total volume of the system can be also a matter of improvement. The volume of the MPHIL, 3  $\mu\text{L}$ , has been chosen as an arbitrary value comparable to operational conditions of commercially available microspectrometers. However, with a proper lens design, able to focus the light in a narrower beam, a sensible volume reduction could be easily achieved by reducing the microchannel's width in the OP, thus reaching submicroliter volumes.

## Conclusions

The novel MPHIL concept has been validated by means of UV spectroscopy detection for protein concentration measurement in a PDMS low cost prototype. The MPHIL has been demonstrated to be suitable for directly determining protein concentration in the  $\mu\text{M}$  range and with a sample volume of only 3  $\mu\text{L}$ , obtaining statistically reliable results. In addition, it has been shown that it is possible to optimize the minimum optical path length (OP), for each system under study and a limit path length of  $L = (9.9 \pm 0.5) \times 10^{-2}$  cm has been estimated for obtaining reliable measurements for glucose isomerase.

The MPHIL concept here presented is compatible with any spectrophotometric measurement in the UV-Vis range and can thus potentially be used for any colorimetric assay, as any conventional spectrometer. Moreover, due to its specific design (a serpentine channel), the system could also operate in a continuous flow regime, making it a good candidate to be used as a detection system for continuous sensing applications. Here, a multispectral measurement coupled to the use of different optical paths allows the simultaneous and accurate detection of more than one analyte, i.e. reactant and product of the reaction. Therefore its potential use could be of high interest for any research and industrial field, ranging from bio-assays and antibody development to the synthesis and testing of new pharmaceutical compounds, where the saving of high added value reagents is a must.

## Acknowledgements

This work has been partly funded by the European Commission (Contract No. 317916) under the LiPhos project (AL & IRR), the MICINN (Spain) projects BIO2010-16800 (JAG) and "Factoría Española de Cristalización" Consolider-Ingenio 2010 (JAG & MCM) and EDRF Funds (JAG & AL).

## Notes and references

<sup>a</sup> Institut de Microelectrònica de Barcelona (IMB-CNM, CSIC), Campus UAB, 08193 Bellaterra, Spain

<sup>b</sup> Laboratorio de Estudios Cristalográficos, IACT (CSIC-UGR). Avda. de las Palmeras, 4. 18100 Armilla, Granada, Spain

1. B. J. S. C. Olson and J. Markwell, in *Current Protocols in Protein Science*, John Wiley & Sons, Inc., 2001.
2. O. H. Lowry, N. J. Rosebrough, A. L. Farr and R. J. Randall, *The Journal of biological chemistry*, 1951, **193**, 265-275.
3. M. M. Bradford, *Analytical Biochemistry*, 1976, **72**, 248-254.
4. P. K. Smith, R. I. Krohn, G. T. Hermanson, A. K. Mallia, F. H. Gartner, M. D. Provenzano, E. K. Fujimoto, N. M. Goeke, B. J. Olson and D. C. Klenk, *Analytical Biochemistry*, 1985, **150**, 76-85.
5. D. R. Reyes, D. Iossifidis, P.-A. Auroux and A. Manz, *Anal. Chem.*, 2002, **74**, 2623-2636.
6. B. Zheng, C. J. Gerdts and R. F. Ismagilov, *Curr. Opin. Struct. Biol.*, 2005, **15**, 548-555.
7. B. Ibarlucea, C. Fernández-Sánchez, S. Demming, S. Büttgenbach and A. Llobera, *Analyst*, 2011, **136**, 3496-3502.
8. J. Wang, *Electrophoresis*, 2002, **23**, 713-718.

9. A. Llobera, R. Wilke and S. Büttgenbach, *Lab Chip*, 2004, **4**, 24-27.
10. J. Vila-Planas, E. Fernández-Rosas, B. Ibarlucea, S. Demming, C. Nogués, J. A. Plaza, C. Domínguez, S. Büttgenbach and A. Llobera, *Nat. Protoc.*, 2011, **6**, 1642-1655.
11. S. Balslev, A. Jorgensen, B. Bilenberg, K. B. Mogensen, D. Snakenborg, O. Geschke, J. Kutter and A. Kristensen, *Lab Chip*, 2006, **6**, 213-217.
12. F. B. Myers and L. P. Lee, *Lab Chip*, 2008, **8**, 2015-2031.
13. X. Muñoz-Berbel, R. Rodríguez-Rodríguez, N. Vigués, S. Demming, J. Mas, S. Büttgenbach, E. Verpoorte, P. Ortiz and A. Llobera, *Lab Chip*, 2013, **13**, 4239-4247.
14. Z. Wang, J. El-Ali, M. Englund, T. Gotsaed, I. Perch-Nielsen, K. B. Mogensen, D. Snakenborg, J. P. Kutter and A. Wolff, *Lab Chip*, 2004, **4**, 372-377.
15. C. L. Bliss, J. N. McMullin and C. J. Backhouse, *Lab Chip*, 2007, **7**, 1280-1287.
16. A. Llobera, R. Wilke and S. Büttgenbach, *Talanta*, 2008, **75**, 473-479.
17. O. C. Jeong and S. Konishi, *Microelectronic Engineering*, 2011, **88**, 2286-2289.
18. C. Con and B. Cui, *Nanoscale Research Letters*, 2013, **8**, 394.
19. C. N. Pace, F. Vajdos, L. Fee, G. Grimsley and T. Gray, *Protein science*, 1995, **4**, 2411-2423.
20. G. L. Long and J. D. Winefordner, *Anal. Chem.*, 1983, **55**, 712A-724A.